Chapter 3
Heaviside World: Excitation and Self-Organization of Neural Fields

Shun-ichi Amari

Abstract Mathematical treatments of the dynamics of neural fields become much simpler when the Heaviside function is used as an activation function. This is because the dynamics of an excited or active region reduce to the dynamics of the boundary. We call this regime the Heaviside world. Here, we visit the Heaviside world and briefly review bump dynamics in the 1D, 1D two-layer, and 2D cases. We further review the dynamics of forming topological maps by self-organization. The Heaviside world is useful for studying the learning or self-organization equation of receptive fields. The stability analysis shows the formation of a continuous map or the emergence of a block structure responsible for columnar microstructures. The stability of the Kohonen map is also discussed.

3.1 Introduction

The dynamics of excitations in a neural field, first proposed by Wilson and Cowan [18], are described by nonlinear partial integro-differential equations. The dynamics include rich phenomena, but sophisticated mathematical techniques are required for solving the equations. Amari [3] analyzed dynamical behavior rigorously by using the Heaviside activation function and showed the existence and stability of a bump solution as well as a traveling bump solution. The Heaviside activation function, instead of a general sigmoid function, makes it possible to analyze the dynamics and to obtain explicit solutions. This framework is called the Heaviside world.

The dynamics of excitation patterns can be reduced to much simpler dynamics of the boundaries of an excitation region [3] in the Heaviside world. In a one-dimensional field, the boundaries of a simple excitation pattern consist of two points, and hence, their dynamics can be described by ordinary differential equations.

S. Amari (✉)
RIKEN Brain Science Institute, Hirosawa 2-1, Wako-shi, Saitama 351-0198, Japan
e-mail: amari@brain.riken.jp

S. Coombes et al. (eds.), *Neural Fields*, DOI 10.1007/978-3-642-54593-1_3,

The boundaries consist of a closed curve in the 2D case. The dynamical behavior of a curve is not so simple but it is still much simpler than the original field equation. See Coombes, Schmit and Bojak [7] and Bressloff [5] for detailed mathematical techniques in the 2D case.

The present Chapter will briefly review the results of pattern dynamics in the Heaviside world. It further demonstrates the dynamics of learning (self-organization) in a neural field, and it elucidates the mechanism of formation of a topological map to fit the environmental information. A model for forming a topological map was proposed by Willshaw and von der Malsburg [16], and it was analyzed by Takeuchi and Amari [15] (see also Amari [4]). Kohonen [11] proposed an engineering model for forming a topological map. We show that the Heaviside world works even in this situation and is applicable to a Kohonen-type map, as was studied in Kurata [12].

3.2 Dynamics of Excitation in a Homogeneous Neural Field

3.2.1 1D 1-Layer Field

We begin with a simplest case of a 1D neural field X with one layer. Let x be a position coordinate of the field. The dynamics are described by

$$\tau \frac{\partial u(x,t)}{\partial t} = -u(x,t) + \int w\left(x - x'\right) f\left[u\left(x', t\right)\right] dx' + s(x,t). \tag{3.1}$$

Here, $u(x,t)$ is the average membrane potential of neurons at a position x at time $t, w\left(x, x'\right)$ is the synaptic connection weight from a position x' to x, $f(u)$ is the activation function such that $z = f(u)$ is the output of neurons at x and $s(x,t)$ is the external stimuli applied to x at t. A threshold is included in the term of external stimuli. The Heaviside world assumes that the activation function is the Heaviside function:

$$f(u) = \begin{cases} 1, & u > 0, \\ 0, & u \le 0. \end{cases} \tag{3.2}$$

We further assume that the field is homogeneous and the connections are symmetric:

$$w\left(x, x'\right) = w\left(\left|x - x'\right|\right). \tag{3.3}$$

First, we shall study the case in which the external stimuli $s(x,t)$ is a constant.

Given $u(x,t)$, the active region of X is defined by

$$A(t) = \{x \mid u(x,t) > 0\}. \tag{3.4}$$

The equation is then rewritten as

$$\tau \frac{\partial u(x,t)}{\partial t} = -u + \int_A w\left(x - x'\right)\, dx' + s. \tag{3.5}$$

It is not easy to solve the equation even in this simplified case. We assume a bump solution such that $u(x,t)$ is positive only in an interval $[x_1, x_2]$; that is, the active or excited region is

$$A(t) = [x_1(t), x_2(t)]\,. \tag{3.6}$$

Note that the boundary points of $A(t)$ satisfy

$$u\left\{x_i(t), t\right\} = 0, \quad i = 1, 2. \tag{3.7}$$

By differentiating this with respect to t, we get

$$\alpha_i \frac{dx_i(t)}{dt} + \frac{\partial u\left(x_i, t\right)}{\partial t} = 0, \tag{3.8}$$

where

$$\alpha_i = \frac{\partial u\left(x_i, t\right)}{\partial x}. \tag{3.9}$$

Therefore, the dynamics of the boundaries are described by

$$\tau \frac{dx_i}{dt} = -\frac{1}{\alpha_i}\left(\int_A w\left(x_i - x'\right) dx' + s\right) \tag{3.10}$$

Let us define

$$W(x) = \int_0^x w\left(x'\right) dx'. \tag{3.11}$$

Thus, we find

$$\int_A w\left(x_i - x'\right)\, dx' = \int_{x_1}^{x_2} w\left(x_i - x'\right)\, dx' \tag{3.12}$$

$$= W\left(x_2 - x_1\right), \tag{3.13}$$

so that

$$\frac{\partial u\left(x_i, t\right)}{\partial t} = \frac{1}{\tau}\left\{W\left(x_2 - x_1\right) + s\right\}. \tag{3.14}$$

The equations of the boundaries have a simple expression:

$$\frac{dx_i(t)}{dt} = -\frac{1}{\tau\alpha_i}\left\{W\left(x_2 - x_1\right) + s\right\}. \tag{3.15}$$

Here, α_1 and α_2 are the slopes of the waveform $u(x,t)$ at x_1 and x_2, and hence,

$$\alpha_1 > 0, \quad \alpha_2 < 0. \tag{3.16}$$

Since α_i are variables depending on the waveform, (3.15) is not a closed expression of the boundaries $x_i(t)$. However, the Heaviside world tells us lots of information on its dynamics.

An equilibrium solution, if it exists, satisfies

$$W\left(x_2 - x_1\right) + s = 0. \tag{3.17}$$

Note that the width of the active region is

$$a(t) = x_2(t) - x_1(t). \tag{3.18}$$

The dynamics have a simple form,

$$\frac{da(t)}{dt} = \frac{1}{\tau\alpha}\{W(a) + s\} \tag{3.19}$$

where

$$\frac{1}{\alpha} = \frac{1}{\alpha_1} - \frac{1}{\alpha_2} > 0. \tag{3.20}$$

The equilibrium solution a satisfies

$$W(a) + s = 0. \tag{3.21}$$

Moreover, by considering the variational equation of (3.19), we see that it is stable when and only when

$$w(a) = W'(a) < 0. \tag{3.22}$$

The waveform of a stable bump solution is explicitly obtained from (3.5) as

$$u(x) = \int_0^a w\left(x - x'\right)\, dx' + s = W(x) + W(a - x) + s. \tag{3.23}$$

Obviously, when $u(x)$ is a stable bump solution, $u(x - c)$ is also a stable bump solution for any constant c. Hence, stable solutions form a one-dimensional set of solutions $\{u(x - c)\}$, which is a line attractor [14].

We studied the case in which s is constant. When s is not constant but has a spatial distribution $s(x)$, a bump moves toward its maximum. Let us assume that an external stimulus $s(x)$ is suddenly applied and consider how the stable bump moves. The velocity of a bump is described by the equation of motion of its center,

$$\frac{1}{2}\frac{d}{dt}(x_1 + x_2) \approx \frac{1}{\tau\alpha_1}\{s(x_2) - s(x_1)\}, \tag{3.24}$$

which depends on the intensity of external stimuli at $s(x_1)$ and $s(x_2)$. The tracking ability of a bump has been analyzed with detail in another solvable model [10, 19], where the Hermite world is used instead of the Heaviside world.

3.2.2 1D Field with Two Layers

We can easily study the equation of a field with two layers, one excitatory and one inhibitory. The equations are

$$\tau_E \frac{\partial u_E(x,t)}{\partial \tau} = -u_E(x,t) + w_{EE} * f[u_E] \\ -w_{EI} * f[u_I] + s_E, \tag{3.25}$$

$$\tau_I \frac{\partial u_I(x,t)}{\partial t} = -u_I(x,t) + w_{IE} * f[u_E] - w_{II} * f[u_I] + s_I, \tag{3.26}$$

where $u_E(x,t)$ and $u_I(x,t)$ are the potentials of excitatory and inhibitory layers, respectively, and the connection weights are $w_{EE}(x)$, $w_{EI}(x)$, $w_{IE}(x)$ and $w_{II}(x)$, depending on the originating layer and terminating layer of excitation and inhibition, with a convolution operator $*$, such as

$$w_{EE} * f[u_E] = \int w_{EE}(x - x') f[u_E(x')] dx'. \tag{3.27}$$

We can analyze the dynamics of the boundary points of active regions in the excitatory and inhibitory layers in a similar manner to obtain a bump solution.

We shall first consider a uniform oscillatory solution in the Heaviside world. The uniform solutions, $u_E(t)$ and $u_I(t)$, do not depend on the position x, so that the equations are simple ordinary differential equations

$$\tau_E \frac{du_E(t)}{dt} = -u_E + W_{EE} f(u_E) - W_{EI} f(u_I) + s_E, \tag{3.28}$$

$$\tau_I \frac{du_I(t)}{dt} = -u_I + W_{IE} f(u_E) + s_I, \tag{3.29}$$

where W_{EE} etc. are, for example,

$$W_{EE} = \int_{-\infty}^{\infty} W_{EE}(x)\,dx. \tag{3.30}$$

We put $W_{II} = 0$ for simplicity's sake. The equations show the population dynamics of excitatory and inhibitory neuron pools proposed by Amari [1, 2] and Wilson and Cowan [18] as a model of neural oscillators. The state space is $\boldsymbol{u} = (u_E, u_I)$. When we use the Heaviside world, we have piecewise linear equations, linear in each quadrant of $\boldsymbol{u}$, determined by $u_E \gtrless 0$, and $u_I \gtrless 0$.

The equations can be written as

$$\tau \frac{d\boldsymbol{u}}{dt} = -\boldsymbol{u} + \bar{\boldsymbol{u}}_k, \quad k = I, II, III, IV \tag{3.31}$$

in the k-th quadrant, where

$$\bar{\boldsymbol{u}}_I = \boldsymbol{s} + \begin{pmatrix} W_{EE} - W_{EI} \\ W_{IE} \end{pmatrix}, \qquad I : u_E > 0,\ u_I > 0, \tag{3.32}$$

$$\bar{\boldsymbol{u}}_{II} = \boldsymbol{s} + \begin{pmatrix} -W_{EI} \\ 0 \end{pmatrix}, \qquad II : u_E < 0,\ u_I > 0, \tag{3.33}$$

$$\bar{\boldsymbol{u}}_{III} = \boldsymbol{s}, \qquad III : u_E < 0,\ u_I < 0, \tag{3.34}$$

$$\bar{\boldsymbol{u}}_{IV} = \boldsymbol{s} + \begin{pmatrix} W_{EE} \\ W_{IE} \end{pmatrix}, \qquad IV : u_E > 0,\ u_I < 0, \tag{3.35}$$

where

$$\boldsymbol{s} = \begin{pmatrix} s_E \\ s_I \end{pmatrix}. \tag{3.36}$$

In the k-th quadrant, the dynamical flow is linear converging to $\bar{\boldsymbol{u}}_k$, but $\bar{\boldsymbol{u}}_k$ is not necessarily in the k-th quadrant (see Fig. 3.1). The direction of the flow changes when $\boldsymbol{u}(t)$ intersects the coordinate axes and enters another quadrant. The dynamical behaviors depend on the positions of $\bar{\boldsymbol{u}}_k$. They are monostable, bistable, and oscillatory, as studied in Amari [1, 2] and Wilson and Cowan [18]. We show the existence and stability of an oscillatory solution in the Heaviside world.

Theorem 1. *A stable oscillation exists when $W_{EE} < W_{EI}$ for an adequate $\boldsymbol{s}$ such that the parallelepiped $\bar{\boldsymbol{u}}_I \bar{\boldsymbol{u}}_{II} \bar{\boldsymbol{u}}_{III} \bar{\boldsymbol{u}}_{IV}$ encircles the origin.*

The existence and stability are clearly shown in Fig. 3.1. In this case $\bar{\boldsymbol{u}}_k$ does not exist in the k-th quadrant and there are no equilibrium states. The oscillatory solution is hence globally stable.

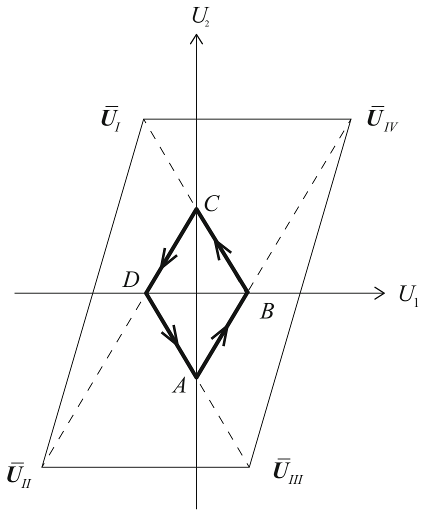

Fig. 3.1 Limit cycle ABCD of oscillation in the two-layers 1D field

In addition to a stationary bump solution, a moving bump solution exists in this field, where such a solution does not exist in a one-layer field. By using moving coordinates, we get

$$\xi = x - ct, \tag{3.37}$$

where c is the velocity of the bump, we have an explicit solution of a moving bump when certain conditions are satisfied. It was analyzed in Amari [3] so that we will not describe it here. The existence of a breathing solution shows the richness of the solutions to these equations. The Heaviside world makes it easier to analyze bump solutions [8, 9].

3.2.3 2D Field of Neural Excitation

The equation of a one layer 2D field is described as

$$\tau \frac{\partial u(\boldsymbol{x}, t)}{\partial t} = -u(\boldsymbol{x}, t) + \int w\left(\boldsymbol{x} - \boldsymbol{x}'\right) f\left[u\left(\boldsymbol{x}', t\right)\right] d\boldsymbol{x}' + s, \tag{3.38}$$

where $\boldsymbol{x} = (x_1, x_2)$ is the coordinates of the field and $\boldsymbol{w}(\boldsymbol{x})$ is a radially symmetric connection function. Let $A(t)$ be an active region in the Heaviside world on which $u(\boldsymbol{x}, t) > 0$. Let $\boldsymbol{x}_A$ be a point on the boundary of A. It satisfies

$$u\left(\boldsymbol{x}_A, t\right) = 0. \tag{3.39}$$

Let us denote the gradient of a waveform by

$$\boldsymbol{\alpha} = \frac{\partial u(\boldsymbol{x}, t)}{\partial \boldsymbol{x}}. \tag{3.40}$$

Then, by differentiating (3.39), we arrive at an equation which describes the motion of the boundary of the excited region:

$$\boldsymbol{\alpha} \cdot \frac{d\boldsymbol{x}_A}{dt} = -\frac{\partial u\left(\boldsymbol{x}_A, t\right)}{\partial t} = -\frac{1}{\tau}\left[\int_A w\left(\boldsymbol{x}_A - \boldsymbol{x}'\right) d\boldsymbol{x}' + s\right]. \tag{3.41}$$

The equilibrium solution satisfies

$$\int_A w\left(\boldsymbol{x}_A - \boldsymbol{x}'\right)\, d\boldsymbol{x}' + s = 0. \tag{3.42}$$

The equilibrium solution having an active region A is written as

$$u(\boldsymbol{x}) = \int_A w\left(\boldsymbol{x} - \boldsymbol{x}'\right) d\boldsymbol{x}' + s. \tag{3.43}$$

When $w(\boldsymbol{x})$ is a radially symmetric function, the radially symmetric equilibrium solution of radius a satisfies

$$u(\boldsymbol{x}) > 0, \quad |\boldsymbol{x}| < a, \tag{3.44}$$

$$u(\boldsymbol{x}) < 0, \quad |\boldsymbol{x}| > 0. \tag{3.45}$$

The equilibrium radius a is obtained from

$$\tilde{W}(a) + s = 0, \tag{3.46}$$

where

$$\tilde{W}(a) = \int_0^{2a} 2rw(r) \cos^{-1} \frac{r}{2a}\, dr. \tag{3.47}$$

However, its stability condition is not easy to determine, because the variational equation for stability has freedom of deformation of A not only in the radial direction, but also of the shape of the boundary circle. The stability was first analyzed in Amari, a Japanese book. See Bressloff and Coombes [6] for later developments. We use polar coordinates (r, θ) to write down the variation of the excited region. Let us write

$$u(r, \theta, t) = u(r, \theta) + \varepsilon v(\theta, t), \tag{3.48}$$

where $u(r, \theta)$ is the equilibrium solution, ε is a small constant and $v(\theta, t)$ denotes the shape of the variation. We use the Fourier expansion of $v(\theta, t)$. The stability condition is given by

$$\lambda_n = \frac{1}{c} \int_0^{2\pi} w\left(2a\left|\cos\frac{\theta}{2}\right|\right) \cos n\theta d\theta - 1 < 0, \quad n = 0, 2, 3, \cdots . \tag{3.49}$$

where

$$c = \int_0^{2\pi} w\left(2a\left|\cos\frac{\theta}{2}\right|\right) \cos\theta d\theta. \tag{3.50}$$

We can extend the idea to a two-layer field having rich dynamical phenomena such as multiple bumps, spiral waves, breathing waves and others. See Chap. 7 in this book. Lu, Sato, and Amari [13] studied traveling bumps and their collisions in a 2D field by simulation. However, the analysis is difficult even in the Heaviside world. See Coombes, Schmidt and Bojak [7] for further developments. Wu and colleagues [10, 19] use another technique of total inhibition, which uses a Gaussian approximation of the bump's shape and its Hermite expansion. This leads us to another world called the Hermite world.

3.3 Self-Organization of Neural Fields

3.3.1 Field Model of Self-Organization

We shall study the self-organization of a 1D homogeneous neural field X which receives inputs from another 1D neural field Y. Fields X and Y have position coordinates x and y, respectively. The input signal to X is assumed to be a bump solution of Y. The neural field X receives stimuli from a bump signal $a(y)$ concentrated around a position y, and they induce a bump solution $u(x)$ of X centered at x. This establishes a correspondence of the positions y and x of two fields Y and X (Fig. 3.2). When Y is a retinal field responsible for the external light stimuli and X is a visual cortex, both being 2D, the correspondence is called a retinotopic map. The map is generated by self-organization of neural fields.

We assume that a bump of Y centered at y' is composed of the activities of neurons at y,

$$a\left(y; y'\right) = a\left(y - y'\right), \tag{3.51}$$

where $a(y)$ is a unimodal waveform of a bump solution. The activities $a(y; y')$ of Y stimulate neurons of X. The connection weight from the position y of Y to the position x of X is written as $s(x, y)$. We also assume that neurons at x receive an inhibitory input of constant intensity a_0 with a synaptic weight $s_0(x)$.

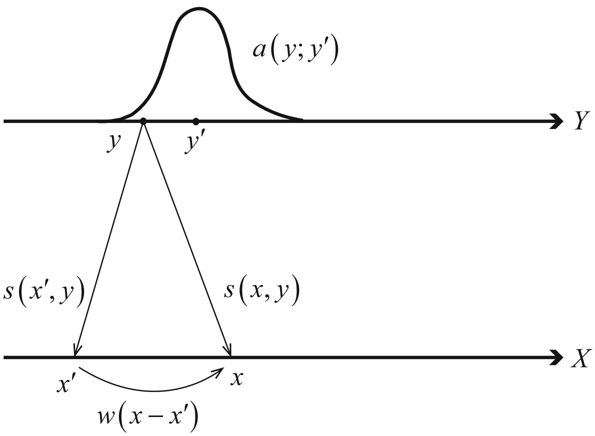

Fig. 3.2 Self-organization of field X by receiving stimuli from field Y

Hence, the total amount of input stimuli given to the neurons at x caused by $a\,(y;\,y')$ is written as

$$S\left(x,y'\right)=\int s(x,y)a\left(y;y'\right)\,dy-s_0(x)a_0. \tag{3.52}$$

The dynamics of excitation in field X is described as follows: Given an input $a\,(y;\,y')$, the neurons at x calculate the inputs $S\,(x,\,y')$ by using (3.52) and $u(x,t)$ changes subject to the dynamics,

$$\tau\frac{\partial u(x,t)}{\partial t}=-u(x,t)+w*f[u]+S\left(x,y'\right). \tag{3.53}$$

The inputs $S\,(x,\,y')$ depend on the connection weights $s(x,\,y)$ and $s_0(x)$. The connection weights are modified in the process of neural activation. This modification is learning or self-organization. We assume a Hebb type of learning rule: Synaptic weight $s\,(x,\,y)$ increases in proportion to the input $a\,(y;\,y')$ when the neuron at x fires and decays with a small time constant. We also assume that a Hebbian rule applies to an inhibitory synapse. For neurons at x, the learning rule is written as

$$\tau'\frac{\partial s\,(x,y)}{\partial t}=-s\,(x,y)+cf\,[u(x,t)]\,a(y;y'), \tag{3.54}$$

$$\tau'\frac{\partial s_0(x)}{\partial t}=-s_0(x)+c'f\,[u(x,t)]\,a_0. \tag{3.55}$$

Here, τ' is a time constant which is much larger than that of the neural excitation, and c and c' are different constants. We also assume that the inhibitory input a_0 is always constant.

A bump excitation of Y randomly appears around the position y'. Let $p\,(y')$ be the probability density of a bump appearing at y'. A bump $a\,(y;\,y')$ continues for a duration which is sufficiently large compared with τ for forming a stable bump in X, but sufficiently small compared with the time constant τ' of learning. Hence, we use the adiabatic approximation and consider the following equation of learning,

$$\tau' \frac{\partial s(x, y)}{\partial t} = -s(x, y) + cf\left[U\left(x, y'\right)\right] a(y; y'), \tag{3.56}$$

$$\tau' \frac{\partial s_0(x)}{\partial t} = -s_0(x) + c' f\left[U\left(x, y'\right)\right] a_0, \tag{3.57}$$

where the current excitation $u(x, t)$ is replaced by the stationary state $U(x, y')$ given rise to by input $a(y; y')$,

$$U\left(x, y'\right) = \int w\left(x - x'\right) f\left[U\left(x', y'\right)\right] dx' + S\left(x, y'\right). \tag{3.58}$$

Considering that τ' is large, before $s(x, y)$ and $s_0(x)$ change substantially, a number of bumps $a(y; y')$ at various y' are randomly chosen. Hence, we further use an averaging approximation for stochastic choices of y'. Let $\langle\cdot\rangle$ denote the average over all possible input bumps $a(y, y')$;

$$\langle f\left[U\left(x, y'\right)\right] a\left(y; y'\right)\rangle = \int p\left(y'\right) f\left[U\left(x, y'\right)\right] a\left(y; y'\right) dy'. \tag{3.59}$$

Accordingly, we get the fundamental equations of learning,

$$\tau' \frac{\partial s(x, y)}{\partial t} = -s(x, y) + c\langle f\left[U\left(x, y'\right)\right] a(y; y')\rangle, \tag{3.60}$$

$$\tau' \frac{\partial s_0(x)}{\partial t} = -s_0(x) + c'\langle f\left[U\left(x, y'\right)\right]\rangle a_0. \tag{3.61}$$

We thus have two important field quantities $U(x, y')$ and $S(x, y')$, both of which depend on $s(x, y)$ and $s_0(x)$ and are hence modified by learning. By differentiating (3.52) and substituting (3.56) and (3.57), we obtain the dynamic equation describing the change of $S(x, y)$,

$$\tau' \frac{\partial S(x, y; t)}{\partial t} = -S(x, y; t) + \int k\left(y - y'\right) f\left[U\left(x, y'\right)\right] p\left(y'\right) dy', \tag{3.62}$$

where we put

$$k\left(y - y'\right) = c \int a\left(y'' - y\right) a\left(y'' - y'\right) dy'' - c' a_0. \tag{3.63}$$

This term shows how two stimuli centered at y and y' overlap. The topology of Y is represented in it (see Fig. 3.3).

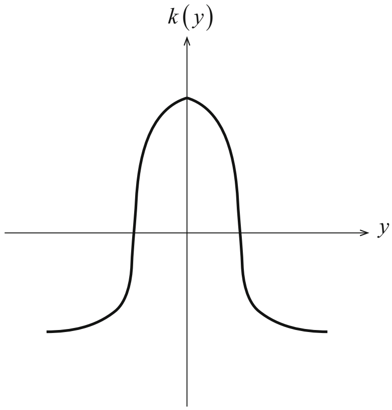

Fig. 3.3 Shape of $k(y)$ defined in (3.63)

Equation (3.62) can be written as

$$\tau' \frac{\partial S\left(x, y'\right)}{\partial t} = -S + k \circ f[U], \tag{3.64}$$

where $\circ$ is another convolution operator defined by

$$k \circ f[U] = \int p\left(y'\right) k\left(y - y'\right) f\left[U\left(x, y'\right)\right] dy'. \tag{3.65}$$

3.3.2 *Dynamics of the Receptive Field*

An equilibrium solution $U\left(x, y'\right)$ is determined by (3.58), depending on $s\left(x, y'\right)$ and $s_0(x)$. Let A be a region on $X \times Y$ such that

$$A = \{(x, y)\,|U(x, y) > 0\}. \tag{3.66}$$

The receptive field $R(x)$ of a neuron at x is a region of Y such that

$$U(x, y) > 0, \quad y \in R(x). \tag{3.67}$$

That is, neurons at x are excited by an input bump around y. We assume that it is an interval,

$$R(x) = \left[r_1(x), r_2(x)\right], \tag{3.68}$$

so that A is bounded by two lines $y = r_1(x)$ and $y = r_2(x)$ (see Fig. 3.4). The size of the receptive field is

$$r(x) = r_2(x) - r_1(x). \tag{3.69}$$

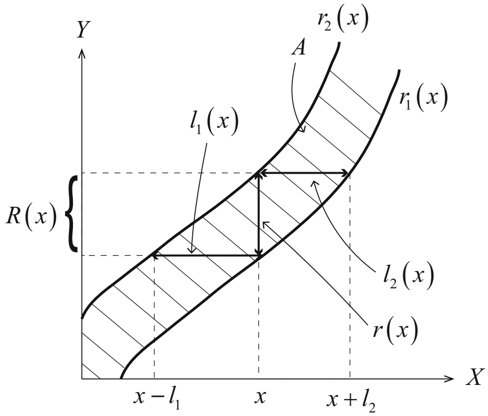

Fig. 3.4 Boundary lines of the active region A in X-Y plane, which represents receptive fields

In contrast, when a bump around y is used, the active region is

$$A(y) = [x_1(y), x_2(y)], \tag{3.70}$$

where

$$x_1(y) = r_2^{-1}(y), \quad x_2(x) = r_1^{-1}(y). \tag{3.71}$$

The length of the active region of X is

$$\bar{x}(y) = r_2^{-1}(y) - r_1^{-1}(y). \tag{3.72}$$

We use the following notations: For an input bump at around $y = r_1(x)$, the excited region is $[x - l_1, x]$ and for an input bump at around $y = r_2(x)$, the excited region is $[x, x + l_2]$. This implies

$$l_1 = x - r_2^{-1}\{r_1(x)\}, \tag{3.73}$$

$$l_2 = r_1^{-1}\{r_2(x)\} - x. \tag{3.74}$$

The equilibrium $U(x, y)$ of (3.58) changes as a result of the change in $S(x, y; t)$ or $s(x, y; t)$ and $s_0(x; t)$. By differentiating (3.58) and using (3.64), we get

$$\tau' \frac{\partial U(x, y; t)}{\partial t} = -S + \tau' \frac{\partial}{\partial t} w * f[U] + k \circ f[U] \tag{3.75}$$

$$= -U + w * f[U] + \tau' \frac{\partial}{\partial t} w * f[U] + k \circ f[U]. \tag{3.76}$$

The dynamical equation governing changes in the receptive field $R(x)$ is gotten by observing the boundary of A, that is $r_1(x)$ and $r_2(x)$. We use

$$\frac{\partial U\left(x, r_i, t\right)}{\partial t} \frac{\partial r_i(x, t)}{\partial t}+\frac{\partial U\left(x, r_i, t\right)}{\partial t}=0 \tag{3.77}$$

to derive the equations of $\partial r_i(x, t)/dt$ in the Heaviside world.

Theorem 2. *The dynamics describing the boundaries of the receptive field is given by*

$$\tau'\left(\alpha_1+\beta_1\right) \frac{\partial r_1(x, t)}{\partial t}-\tau' \beta_1 \frac{\partial r_2\left(x-l_1, t\right)}{\partial t}=-W\left(l_1\right)-K(r)-s, \tag{3.78}$$

$$\tau'\left(\alpha_2-\beta_2\right) \frac{\partial r_2(x, t)}{\partial t}+\tau' \beta_2 \frac{\partial r_1\left(x+l_2, t\right)}{\partial t}=-W\left(l_2\right)-K(r)-s, \tag{3.79}$$

where $l_i=l_i(x, t)$, $r=r(x, t)$ *and*

$$W(l)=\int_0^l w(x)\, dx, \tag{3.80}$$

$$K(r)=\int_0^r k(y)\, dy, \tag{3.81}$$

$$\alpha_i=\frac{\partial U\left(x, r_i, t\right)}{\partial y}, \quad i=1,2 \tag{3.82}$$

$$\beta_1=-w\left(l_1\right) \Bigg/ \frac{\partial r_2\left(x-l_1, t\right)}{\partial x}, \tag{3.83}$$

$$\beta_2=-w\left(l_2\right) \Bigg/ \frac{\partial r_1\left(x+l_2, t\right)}{\partial x}. \tag{3.84}$$

Proof. To evaluate $\partial U/\partial t$ at $y=r_1$, we first calculate $K \circ f[U]$ at $r_1(x)$. We easily have

$$\int k\left(r_1-y'\right) f\left[U\left(x, y'\right)\right] dy'=\int_{r_1}^{r_2} k\left(r_1-y'\right) dy'=K\left(r_2-r_1\right), \tag{3.85}$$

where we have used $K(r)=K(-r)$ and we have assumed that the distribution of input stimuli of Y is uniform, $p\left(y'\right)=1$, by normalizing the length of Y equal to 1. Similarly, we have

$$\int w\left(x-x'\right) f\left[U\left(x', r_1\right)\right] dx'=\int_{x-l_1}^x w\left(x-x'\right)=W\left(l_1\right). \tag{3.86}$$

Hence,

$$\frac{\partial}{\partial t} w * f[U]=w\left(l_1\right) \frac{\partial l_1}{\partial t} \tag{3.87}$$

at $y = r_1$. Therefore,

$$\tau' \frac{\partial U(x, r_1)}{\partial t} = \tau' w(l_1) \frac{\partial l_1}{\partial t} + W(l_1) + K(r) + s. \tag{3.88}$$

We need to evaluate $w(l_1)\, \partial l_1 / \partial t$. By differentiating

$$r_2(x - l_1) = r_1(x) \tag{3.89}$$

with respect to t, we get

$$\frac{\partial r_1(x)}{\partial t} = \frac{\partial r_2(x - l_1)}{\partial t} - \frac{\partial r_2(x - l_1)}{\partial x} \frac{\partial l_1(x)}{\partial t}. \tag{3.90}$$

We substitute $\partial l_1 / \partial t$ obtained from (3.90) in (3.88), and we finally get (3.78). Calculations at $y = r_2$ yield (3.79).

3.3.3 Equilibrium Solution of Learning

The equilibrium solutions $\bar{U}$ and $\bar{S}$ of the dynamics of learning are derived by putting $\partial S / \partial t = 0$ in (3.62). They satisfy the following equations

$$\bar{U}(x, y) = w * f[\bar{U}] + \bar{S}, \tag{3.91}$$

$$\bar{S}(x, y) = k \circ f[\bar{U}], \tag{3.92}$$

In order to understand the formation of a topological map from Y to X and its stability, we consider a simple situation: We eliminate the boundary conditions by assuming that both Y and X are rings, where we normalize the lengths of the rings equal to 1, $L_X = L_Y = 1$.

We then search for an equilibrium solution of (3.78) and (3.79). Since the equilibrium solution satisfies

$$W(l_1) + K(r) + s = 0, \tag{3.93}$$

$$W(l_2) + K(r) + s = 0, \tag{3.94}$$

it is easy to see that

$$l_1(x) = l_2(x) = l(x). \tag{3.95}$$

As can be seen from Fig. 3.4, we get

$$l(x) = l\{x + l(x)\}, \quad \mod 1. \tag{3.96}$$

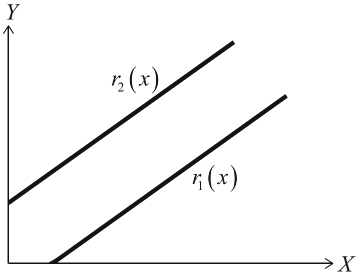

Fig. 3.5 Continuous map from Y to X

When $l(x)$ is continuous, it has only a constant solution (see Takeuchi and Amari [15]),

$$l(x) = \bar{l}. \tag{3.97}$$

This implies

$$r(x) = \bar{r} \tag{3.98}$$

and hence $r_2(x)$ is a shift of $r_1(x)$, $r_2(x) = r_1(x) + \bar{r}$.

The solution

$$r_1(x) = x + c, \tag{3.99}$$

$$r_2(x) = x + c + \bar{r} \tag{3.100}$$

is an equilibrium for any constant c. This gives a natural correspondence between Y and X (Fig. 3.5). Now, let us study its stability.

However, first, there is a delicate problem as to whether other equilibrium solutions exist or not. When $\bar{l}$ is a rational number,

$$\bar{l} = \frac{m}{n}, \tag{3.101}$$

we find that

$$r_1(x) = x + c + g(x) \tag{3.102}$$

$$r_2(x) = x + c + \bar{r} + g(x) \tag{3.103}$$

is also an equilibrium solution, where $g(x)$ is a periodic function with a period $1/n$. This is a rippled solution, but we may disregard the ripple when n is large.

3.3.4 Stability of the Equilibrium Solution

We shall study the stability of the simple equilibrium solution (3.99), (3.100) in order to check if the continuous topological mapping is stable. We put $c = 0$ and perturb the solution as

$$r_1(x,t) = x + \varepsilon v_1(x,t) \tag{3.104}$$

$$r_2(x,t) = x + \bar{r} + \varepsilon v_2(x,t) \tag{3.105}$$

where ε is a small constant. The variational equation is

$$\tau'(\alpha+\beta)\frac{\partial v_1(x,t)}{\partial t} - \tau'\beta\frac{\partial v_2\left(x-\bar{l},t\right)}{\partial t} = \beta\left\{v_2\left(x-\bar{l},t\right) - v_1(x,t)\right\} - k\left(\bar{r}\right)\left\{v_2(x,t) - v_1(x,t)\right\}, \tag{3.106}$$

$$\tau'(\alpha+\beta)\frac{\partial v_2(x,t)}{\partial t} - \tau'\beta\frac{\partial v_1\left(x+\bar{l},t\right)}{\partial t} = -\beta\left\{v_2(x,t) - v_1\left(x+\bar{l},t\right)\right\} + k\left(\bar{r}\right)\left\{v_2(x,t) - v_1(x,t)\right\}, \tag{3.107}$$

where

$$\alpha = \frac{\partial \bar{U}\left(x, r_1(x)\right)}{\partial y}, \quad \beta = -w\left(\bar{l}\right) \Big/ \frac{dr_1(x)}{dt}\,. \tag{3.108}$$

We expand v_1 and v_2 in a Fourier series,

$$v_1(x,t) = \sum V_1(n,t)\exp\left\{i2n\pi x\right\}, \tag{3.109}$$

$$v_2(x,t) = \sum V_2(n,t)\exp\left\{i2n\pi x\right\}. \tag{3.110}$$

The variational equation then separates for every n, giving ordinary differential equations for each $n = 0, 1, \cdots$:

$$\tau' A_n \frac{d}{dt}\begin{bmatrix} V_1(n,t) \\ V_2(n,t) \end{bmatrix} = B_n \begin{bmatrix} V_2 \\ V_2 \end{bmatrix}, \quad n = 0, 1, \cdots, \tag{3.111}$$

where

$$A_n = \begin{bmatrix} \alpha+\beta & -\beta\bar{z}_n \\ -\beta z_n & \alpha+\beta \end{bmatrix}, \quad B_n = \begin{bmatrix} k-\beta & \beta\bar{z}_n - k \\ \beta z_n - k & k-\beta \end{bmatrix}, \tag{3.112}$$

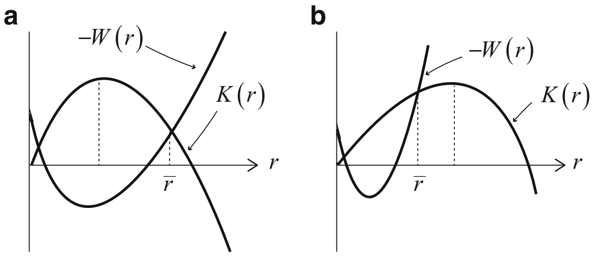

Fig. 3.6 Stability of continuous solutions: (**a**) stable, (**b**) unstable

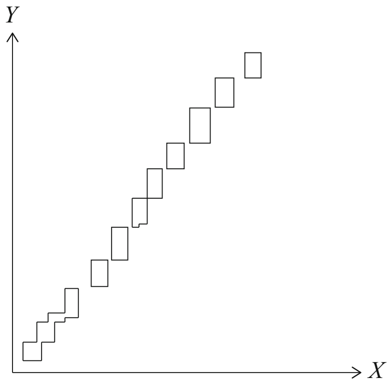

Fig. 3.7 Simulation result of block formation in unstable case

$B_n = \exp\left\{i2n\pi\bar{l}\right\}$. The stability depends on the eigenvalues λ:

$$\det|\lambda A_n - B_n| = 0. \tag{3.113}$$

We shall omit the detailed derivation, since they are rather technical (see Takeuchi and Amari [15]).

Theorem 3. *The equilibrium solution is stable when and only when*

$$k(\bar{r}) < 0, \quad w(\bar{l}) < 0. \tag{3.114}$$

Roughly speaking, the continuous map is stable when the length of the receptive field $\bar{r}$ is wider than the length $\bar{l}$ of the active region of the input field, and is unstable otherwise. (See Fig. 3.6a for the stable and Fig. 3.6b for unstable solutions.) We can also analyze the stability of a rippled solution, but the result is the same.

The variational analysis does not tell what will happen in the unstable case. Computer simulations show that both X and Y are divided into discrete blocks, and there exists a mapping from a block of Y to a block of X (see Fig. 3.7). The topology of X and Y is preserved in the discretized sense. When an input bump is in a block of Y, then all the neurons in the corresponding block of X are excited. This might explain the mechanism behind the formation of microscopic columnar structures observed in the cerebrum. This mechanism is important when

Y has more dimensions than X. For example, let us consider the case where Y is a set of stimuli given to the retina. We assume that a bar with an arbitrary orientation is presented at any position on the retina. The set of stimuli is three-dimensional, having two dimensions corresponding to the positions of a bar and one dimension corresponding to the orientation of the bar. In this case, $Y = \boldsymbol{R}^2 \times S^1$. Such stimuli are mapped to the visual cortex $X = \boldsymbol{R}^2$. It is known that X decomposes into an aggregate of blocks called a column. The position of a bar is mapped to the position of blocks of X in a discretized manner and keeps the topography. There is a microstructure inside a block such that the orientation of the bar is continuously mapped inside a columnar block. This is the wisdom of nature expressed through evolution. Our theory might explain it.

When $p(y')$ is not uniform, some part of Y is stimulated more frequently than the other part. It is plausible that a frequently stimulated part of Y has a finer representation occupying a larger part of X. This effect is analyzed in [4].

3.3.5 Kohonen Map

Kohonen [11] proposed a neural mechanism of self-organization, which generates a topological map from the space of input signals to a neural field. It is an engineering model simplifying the Willshaw and Malsburg model [17] such that the dynamics of neural excitation are omitted. This mechanism is applicable to various engineering problems and is known as Kohonen's SOM (self-organizing map).

The input signal field Y gives a vector-valued output $\boldsymbol{a}(y')$, when position y' is activated. In the previous case, this is a bump $a(y; y')$ in Y. Here, we regard this as a vector $\boldsymbol{a}(y')$ whose components are $a(y; y'),\ y \in Y$. In our previous case, Y is 1-dimensional and the activation vector is $\boldsymbol{a}(y') = a(y; y')$. We regard the distribution $a(y; y')$ over $y \in Y$ as a vector $\boldsymbol{a}(y')$. The output layer X is a neural field, typically 2-dimensional. A neuron at position x has a connection weight vector $\boldsymbol{s}(x)$. When it receives an input signal $\boldsymbol{a}(y')$, it calculates the inner product of $\boldsymbol{s}(x)$ and $\boldsymbol{a}(y')$, obtaining

$$u\left(x, y'\right) = \boldsymbol{s}(x) \cdot \boldsymbol{a}\left(y'\right) = \int s(x, y) a\left(y; y'\right) dy, \tag{3.115}$$

where we have put $\boldsymbol{s}(x) = s(x, y)$. The neurons of X are not recurrently connected and no dynamics of excitation take place in X in the Kohonen model. Instead, the activation $f[u(x)]$ of the neural field is decided by a simple rule stated in the following. The neuron at position x is said to be the winner when it has the highest value of $u(x, y')$ when a stimulus $\boldsymbol{a}(y')$ is applied. The winner neuron $\bar{x}$ corresponding to input $\boldsymbol{a}(y')$ is hence defined by

$$\bar{x}(\boldsymbol{a}) = \arg\max_{x} u\left(x, \boldsymbol{a}\left(y'\right)\right). \tag{3.116}$$

When the absolute values of vector $\boldsymbol{a}$ and weight $\boldsymbol{s}$ are normalized to 1, the winner is the neuron whose weight $\boldsymbol{s}(x)$ is closer to the input pattern vector $\boldsymbol{a}$.

We then define a neighborhood of a neuron x by using a distance function $d\,(x, x')$. The neighborhood $N(x)$ of x is a set of positions x' given by

$$N(x) = \left\{x' \left| d\left(x, x'\right) \le c \right.\right\} \tag{3.117}$$

for a constant c. When $\bar{x}$ is the winner for input $\boldsymbol{a}$, the neurons in the neighborhood of $\bar{x}$ are excited. Hence, we have

$$f\left[u\left(x, y'\right)\right] = \begin{cases} 1, \; x \in N\left(\bar{x}\right), \\ 0, \; \text{otherwise.} \end{cases} \tag{3.118}$$

This is the Heaviside world, although the excited neurons are determined by this simple rule, not by recurrent dynamics.

The connection weight vector $\boldsymbol{s}(x)$ of an excited neuron $x \in N\,(\bar{x})$ changes according to a Hebb-like rule: The weight vector $\boldsymbol{s}(x)$ moves toward the input $\boldsymbol{a}$, and then, the normalization takes place. Hence, the rule is written as

$$\boldsymbol{s}(x) \to \frac{\boldsymbol{s}(x) + \varepsilon \boldsymbol{a}}{|\boldsymbol{s}(x) + \varepsilon \boldsymbol{a}|} \approx \{1 - \varepsilon\, |\boldsymbol{a} \cdot \boldsymbol{s}|\}\, \boldsymbol{s} + \varepsilon \boldsymbol{a} \tag{3.119}$$

for small constant ε, when x belongs to the neighborhood $N\,\{\bar{x}(\boldsymbol{a})\}$. The weight vectors outside the neighborhood do not change.

We use the continuous time version of learning and rewrite the dynamics of $\boldsymbol{s}(x)$ in the differential equation,

$$\tau' \frac{d\boldsymbol{s}(x)}{dt} = -\boldsymbol{s} + \varepsilon \langle \left\{\boldsymbol{a}\left(y'\right) - \boldsymbol{a}\left(y'\right) \cdot \boldsymbol{s}(x)\right\} \boldsymbol{s}(x) \rangle. \tag{3.120}$$

Here, we use the adiabatic assumption such that the time constant τ' of learning is sufficiently small compared with the duration in which a randomly chosen stimulus $\boldsymbol{a}\,(y')$ is applied.

Let us see if a topological map between Y and X is formed stably by the Kohonen SOM mechanism. K. Kurata analyzed this problem in his doctoral dissertation and in a Japanese paper [12]. He proved that, when Y and X are one-dimensional, the continuous topological map $y = r(x)$ is always neutrally stable. He also analyzed the case when Y is one-dimensional and X is two-dimensional. Then, self-organization embeds Y as a curve in X. He showed that there are three possibilities depending on the sizes of the abscissa and ordinate of X.

Consider the map

$$Y \to X: \; x_1(y) = y, \tag{3.121}$$

$$x_2(y) = c. \tag{3.122}$$

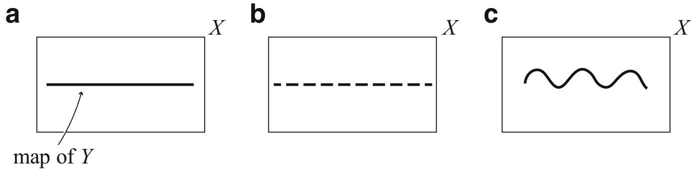

Fig. 3.8 Stability of Kohonen map: (**a**) 1-D Y is stably embedded, (**b**) unstable and block structure emerges, (**c**) unstable and wave emerges

This is an equilibrium solution (Fig. 3.8a). It is stable or unstable, depending on the parameters. There are two types of instability. In one case, it is unstable in the vertical direction, so that a wave pattern emerges (see Fig. 3.8c). The second case is that it is unstable in the horizontal direction, so that the block structure emerges (see Fig. 3.8b). This is an interesting but regrettably not well known result.

3.4 Conclusions

The study of dynamics of a neural field is currently a 'hot' research topic. However, its mathematical treatment is difficult. When one approximates the activation function by the Heaviside function, the dynamics can be dramatically simplified and one can find exact results in some cases. This is the Heaviside world, in which the dynamics of an active region can be analyzed in terms of the dynamics of its boundary. The Heaviside world recaptures previous important results including the formation of a topological (topographic) map in the cortex.

The Heaviside world plays an important role in the analysis of topographic map formation. We analyzed a one-dimensional mapping, and proved that a topological map is unstable under a certain condition. In such a case, a block structure or micro-columnar structure emerges. This analysis may account for the formation of columnar microstructures in the visual cortex.

References

1. Amari, S.: Characteristics of randomly connected threshold-element networks and network systems. Proc. IEEE **59**(1), 35–47 (1971)
2. Amari, S.: Characteristics of random nets of analog neuron-like elements. IEEE Trans. Syst. Man Cybern. (SMC) **2**(5), 643–657 (1972). (Also Vemri, V. (ed.): Artificial Neural Networks Theoretical Concepts. IEEE Computer Society (1988))
3. Amari, S.: Dynamics of pattern formation in lateral-inhibition type neural fields. Biol. Cybern. **27**, 77–87 (1977)
4. Amari, S.: Topographic organization of nerve fields. Bull. Math. Biol. **42**, 339–364 (1980)
5. Bressloff, P.C.: Spatiotemporal dynamics of continuum neural fields. J. Phys. A **45**, 1–109 (2012)

6. Bressloff, P.C., Coombes, S.: Neural ‘bubble’ dynamics revisited. Cogn. Comput. **5**, 281–294 (2013)
7. Coombes, S., Schmidt, H., Bojak, I.: Interface dynamics in planar neural field models. J. Math. Neurosci. **2**, 9 (2012)
8. Folias, S.E.: Nonlinear analysis of breathing pulses in synaptically coupled excitable neural activity. J. Comput. Neurosci. **11**, 121–134 (2011)
9. Folias, S.E., Bressloff, P.C.: Breathing pulses in an excitatory neural network. SIAM J. Appl. Dyn. Syst. **3**, 378–407 (1974)
10. Fung, C.A., Wong, M., Wang, H., Wu, S.: Dynamical synapses enhance neural information processing: Gracefulness, accuracy and mobility. Neural Comput. **24**, 1147–1185 (2012)
11. Kohonen, T.: Self-organized formation of topologically correct feature maps. Biol. Cybern. **43**, 59–69 (1982)
12. Kurata, K.: Formation of information representation by self-organization. In: Japanese Association of Industrial Technology (eds.) Basics of Neurocomputing, chap. 5. Japanese Association of Industrial Technology, Tokyo (1989). in Japanese
13. Lu, Y., Sato, Y., Amari, S.: Travelling bumps and their collisions in a two-dimensional neural field. Neural Comput. **23**, 1248–1260 (2011)
14. Seung, H.S.: Continuous attractors and oculomotor control. Neural Netw. **11**, 1253–58 (1998)
15. Takeuchi, A., Amari, S.: Formation of topographic maps and columnar microstructures. Biol. Cybern. **35**, 63–72 (1979)
16. von der Malsburg, C.: Self-organization of orientation sensitivity and columns in the visual cortex. Kybernetik **14**, 85–100 (1973)
17. Willshaw, D.J., von der Malsburg, C.: How patterned neural connections can be set up by self-organization. Proc. R. Soc. B **194**, 431–445 (1976)
18. Wilson, H.R., Cowan, J.D.: Excitatory and inhibitory interactions in localized populations of model neurons. Biophys. J. **12**, 1–24 (1972)
19. Wu, S., Amari, S.: Computing with continuous attractors: Stability and on-line aspects. Neural Comput. **17**, 2215–2239 (2005)